Polyurethane/Acrylate Hybrids: Effects of the Acrylic Content and Thermal Treatment on the Polymer Properties

Pablo J. Peruzzo,[1] Pablo S. Anbinder,[1,2] Oscar R. Pardini,[1] Carlos A. Costa,[3] Carlos A. Leite,[3] Fernando Galembeck,[3] Javier I. Amalvy[1,2]

[1]*Polymeric Materials and Nanomaterials Group, Instituto de Investigaciones Fisicoquímicas Teóricas y Aplicadas, UNLP-CCT La Plata, Consejo Nacional de Investigaciones Científicas y Técnicas, Universidad Nacional de La Plata, Diag. 113 y 64 CC 16 Suc. 4, B1904DPI, La Plata, Argentina*
[2]*Polymeric Materials and Nanomaterials Group, LIMF, Carrera Ingeniería en Materiales, Facultad de Ingeniería, Universidad Nacional de La Plata, Calle 116 y 48, B1900TAG, La Plata, Argentina*
[3]*Instituto de Química, Universidade Estadual de Campinas, Caixa Postal 6154, Unicamp, IQ, P.O. Box 6154, 13083-970 Campinas SP, Brazil*

Received 5 June 2009; accepted 15 November 2009
DOI 10.1002/app.31795
Published online 27 January 2010 in Wiley InterScience (www.interscience.wiley.com).

ABSTRACT: Polyurethane (PU)/acrylate hybrids with different acrylic contents (10, 30, 50, 70, and 90 wt %) were prepared by the polymerization of acrylic monomers in the presence of preformed PU chains with polymerizable terminal vinyl groups. Films obtained by the casting of polymer dispersions before and after thermal annealing were characterized by dynamic light scattering, Fourier transform infrared spectroscopy, transmission electron microscopy (TEM), TEM electron energy-loss spectroscopy, differential scanning calorimetry, and gel fraction determination. Small-angle X-ray scattering (SAXS), wide-angle X-ray scattering, mechanical properties testing, atomic force microscopy, water contact angle testing, Buchholz hardness testing, and roughness testing of the films were also performed. The effects of the acrylic content and thermal treatment on the structure and properties were determined. TEM showed that a core–shell morphology was formed during polymerization. When the acrylic content increased, smaller particles without core–shell morphologies were observed. TEM energy-loss spectroscopy studies confirmed this observation. Systems with up to 50 wt % acrylic component were homogeneous, as determined by SAXS, before and after thermal annealing. An attempt to incorporate a higher amount of acrylic component led to phase-separated materials with a different morphology and, therefore, different properties. The relationship between the acrylic content and properties did not follow linear behavior. © 2010 Wiley Periodicals, Inc. J Appl Polym Sci 116: 2694–2705, 2010

Key words: core–shell polymers; dispersions; phase separation; polyurethanes

INTRODUCTION

Aqueous polyurethane (PU) dispersions are widely used for applications such as adhesives and coatings for various materials, for example, textiles, metals, plastics, and wood. PUs are known for their excellent mechanical properties, and depending on their structure, it is possible to have hard or tough systems with flexibility (even at low temperatures). This characteristic is attributed to the combination of hard segments (HSs) and soft segments (SSs) in the polymer and the hydrogen bonding between the urethane linkages of different chains. PU films show excellent elasticity and abrasion resistance and a superior low-temperature impact resistance. In addition, they represent a major trend of PU development because of the increasing concern about environmental pollution and health and safety risks.[1] However, the interest in new materials that have intimate combinations of incompatible components at the nanoscale level has attracted significant attention because these materials offer prospects for new and synergistic properties. For example, mixtures of PU with polyacrylate (AC) systems can be used.[2,3] However, the simple blending of AC dispersions with PU dispersions often leads to films of lower quality, which is attributed to a low compatibility of both components. The formation of hybrid systems, on the other hand, leads to a better mixing of components by the suitable combination of the properties of both polymers. Several trials toward this objective have been described during recent decades, so there are examples of syntheses of polyacrylic/PU hybrid dispersions and morphology characterizations of these systems in the existing literature.[4–13] A useful synthetic method is the polymerization of acrylic monomers in the presence of preformed PU

Correspondence to: J. I. Amalvy (jamalvy@inifta.unlp.edu.ar or javier.amalvy@ing.unlp.edu.ar).

Contract grant sponsors: CICPBA, Agencia Nacional de Promoción Científica y Tecnológica and LNLS - Brazilian Synchrotron Light Laboratory/MCT (proposal D11A-SAXS #3443/04) (partially).

chains with polymerizable terminal vinyl groups; this leads to products known as PU/acrylate or acrylic/PU hybrids.[14]

In these hybrid systems, the two polymers may form a homogeneous blend within the particle, or nanophase–microphase separation may occur. In practice, the product of the polymerization of acrylic monomers in the presence of a premade polymer dispersion (e.g., an acrylic emulsion seed or PU dispersion) is characterized by one of a broad range of multiphase particles in which partial or complete phase separation has occurred (core–shell, lobed, inverted core–shell, etc.).[15]

It is generally understood that the chemical species occupying the shell region of the emulsion particles is preferentially located in the surface layer of the cast films after the process of coalescence of emulsion particles and film formation.[16] Waterborne coatings are most prone to this, and this is sometimes intensified by imperfect film formation due to the process of coalescence. So, the films are clearly heterogeneous in a nanoscopic–microscopic sense.

In addition, the curing process (thermal annealing) can originate heterogeneities, such as voids and low crosslinked zones, in the solid film. This affects the phase-separation behavior and the eventual morphology. Even seemingly insignificant structural changes in individual polymers can cause significant differences in the phase behavior.[17,18]

It is well established that the physical and mechanical properties of polymers depend not only on the chemical structure but also on their morphology. The elasticity, toughness, and other physical properties of these materials are determined largely by the degree of phase separation, interconnectivity of the HSs, nature of the segment interface, and mixing of the HS in the SSs.[19] Systems that exhibit a very low degree of phase separation often exhibit worse properties than those with a higher degree of separation;[20] however, depending on the nature of SSs, results suggest that exceeding a certain degree of phase separation leads to inferior properties. Adhesion between HSs and SSs also plays an import role, and it has been suggested that the adhesive process occurs primarily through physical bonds.[21] The importance of hydrogen bonding in determining the physical properties is well known, and the incorporation of increasing amounts of AC to PU or vice versa produces important changes in the polymer properties.

The characterization of polymer morphology is very important from a practical point of view. In many technical applications, the observation of changes in polymer morphology allows the best polymer composition and preparation conditions to be chosen and the achievement of desired properties in the final product.

However, there have not been many reports in the published literature about the preparation and properties of these hybrid materials in all ranges of concentrations (from pure PU to pure AC). In addition, there have been few attempts to study the effect of thermal annealing on the phase behavior and morphology of these systems over all ranges of acrylic content.

In previous studies, we examined the kinetic reactions of these systems,[22] and we reported the characterization of samples where the acrylic content was varied from 0 to 50 wt %. Higher amounts of acrylic components led to coagulation, and no film-forming systems were obtained.[23] These film-forming polymeric systems are suitable for the formulation of gloss top coatings.[24]

This article describes the most important aspects of the synthesis of hybrid acrylic/PU systems by the polymerization of acrylic monomers in the presence of preformed PU chains containing polymerizable terminal vinyl groups. To extend our studies, the glass transition of the acrylic component was adjusted to obtain film-forming systems in all ranges of composition (from pure PU to pure AC) and with a surfactant to prevent coagulation at higher acrylic contents. Here, the emphasis was placed on the comparative properties of the hybrid polymer films obtained from purified dispersions, before and after annealing, to study the effect of the thermal treatment on their structural characteristics, according to the acrylic content.

EXPERIMENTAL

Materials

Methyl methacrylate (MMA) and *n*-butyl acrylate (*n*-BuA) were technical grade and were distilled before use. Methacrylic acid (MAA; Fluka, Buenos Aires, Argentina), isophorone diisocyanate (IPDI; Aldrich, Buenos Aires, Argentina), 2-hydroxyethyl methacrylate (HEMA; Aldrich), potassium persulfate (Anedra), hydrazine monohydrate (HZN; Aldrich), dibutyltin dilaurate (DBTDL; Aldrich), triethylamine (TEA; UVE), and sodium dodecyl sulfate (SDS; Anedra) were analytical grade and were used as received. Polypropylene glycol 1000 (PPG1000; Voranol 2110, Buenos Aires, Argentina) was dried and degassed at 80°C at 1–2 mmHg, before use. Dimethylol propionic acid (DMPA; Aldrich) was dried at 100°C for 2 h in an oven.

Polymer dispersion synthesis

PU was synthesized according to a prepolymer mixing process by the polyaddition of IPDI, polypropylene glycol, HEMA, and 2,2-bis(hydroxymethyl)propionic

TABLE I
Recipe for the Synthesis of the PU Dispersion

Component	Weight (g)	Moles
	Prepolymer reaction	
IPDI	108	0.49
PPG1000	147.23	0.15
DMPA	14.81	0.11
HEMA	12.65	0.10
DBTDL	0.42	
	Neutralization reaction	
TEA	11.17	0.11
	Dispersion and chain-extension reaction	
HZN	5.75	0.18
Water	700	

acid. The PU anionomer with 2-ethoxymethacrylate terminal groups was dispersed in water containing a chain extender (hydrazine) with prior neutralization of carboxylic acid groups with TEA. A typical base formulation of PU used in this article is given in Table I. An emulsion polymerization with an MMA/*n*-BuA/MAA (45/53/2% w/w) mixture was performed in the presence of SDS as an emulsifier (2% w/w on an acrylic monomer base). The polymerization led to the formation of colloidal dispersions of the PU/acrylic hybrids. More experimental details on the preparation of these polymers were described in a previous article.[23] Shorthand notation is used in this article to describe the hybrid systems. For example, H90 : 10 denotes the hybrid system prepared with 90 wt % PU and an acrylic feed of 10 wt %. The pure acrylic dispersion (AC) was prepared by the emulsion polymerization of an MMA/*n*-BuA/MAA mixture in the same way as used for the PU/acrylic hybrids with 2% SDS in the monomer base as an emulsifier. The polyurethane polymerized dispersion (PUpol) was prepared in the same way as the hybrid systems without the addition of the acrylic monomers. Both polymers were used as reference materials for comparison with the hybrid systems (Table II).

Polymer dispersion cleaning

The dispersions were cleaned before analysis with Spectra/Por Biotech poly(vinylidene difluoride) dialysis membranes 15 mm in diameter and with a molecular weight cutoff of 1,000,000 Da to eliminate residual monomers, initiators, and water-soluble compounds, as they could interfere in the analytical techniques.

Film formation

We prepared the films by casting the dispersions on a Teflon substrate by evaporating the water at 30°C. Samples were thermally treated (cured) at 60°C for 48 h to allow complete coalescence.

Characterization

The particle sizes of the dispersions were determined by dynamic light scattering (DLS) with a Malvern 4700 instrument (Worcestershire, UK). This technique gives an intensity-weighted average particle size:

$$d_{\text{int avg}} = \Sigma(n_i I_i d_i)/\Sigma(n_i I_i)$$

where I_i is the intensity of light scattered from n_i particles of diameter d_i being close to the z-average particle size (d_z):

$$d_z = \Sigma(n_i d_i^7)/\Sigma(n_i d_i^6)$$

The gel fraction was determined by Soxhlet extraction with tetrahydrofuran as a solvent during a 24-h period. The cartridge (Whatman 1, weight W_1) was loaded with about 1 g of dry polymer (weight W_2), and then, the extraction was carried out. The cartridge was dried in a ventilated oven at 60°C and weighed again (weight W_3). The amount of insoluble material (the gel fraction) was calculated as follows:

$$\text{Gel fraction} = [(W_3 - W_1)/(W_2 - W_1)] \times 100$$

Fourier transform infrared (FTIR) spectra were measured in the transmission mode with a Nicolet 380 FTIR spectrometer (Thermo Fisher Scientific, Waltham, MA). Films of the polymers were prepared by spontaneous evaporation at room temperature of a diluted dispersion placed on a CaF_2 window. The number of scans per experiment was 64.

Transmission electron microscopy (TEM) studies were performed with a JEOL JEM 1200 EX II instrument (Tokyo, Japan). Dilute dispersions were dried onto carbon-coated copper grids covered with Formvar and without a metal coating. To improve the contrast, some samples were stained with 1%

TABLE II
Typical Base Formulation of Different Polymers Prepared in This Study

System	Acrylic content (wt %)	PU dispersion (g)	Acrylic monomers (g)[a]	SDS (g)	Water (g)
PUpol	0	100	—	—	—
H90 : 10	10	90	3	0.06	7
H70 : 30	30	70	9	0.18	21
H50 : 50	50	50	15	0.30	35
H30 : 70	70	30	21	0.42	49
H10 : 90	90	10	27	0.54	63
AC	100	0	30	0.60	70

[a] *n*-BuA/MMA/AA (53:45:2 wt%).

TABLE III
Particle Size and Gel Fraction of the Systems Prepared in This Study

Sample	Diameter (nm)	Gel fraction (%)
PU	94	0
PUpol	114	84
H90 : 10	165	91
H70 : 30	159	94
H50 : 50	134	87
H30 : 70	120	92
H10 : 90	107	91
AC	80	0

phosphotungstic acid for 40 s and then air-dried. Electron spectroscopy imaging in the TEM, based on electron energy-loss spectroscopy, were performed with a Zeiss CEM902 microscope. Other experimental details regarding TEM were presented elsewhere.[25,26]

Differential scanning calorimetry (DSC) were performed with a Shimadzu (Kyoto, Japan) DSC-60 instrument between −100 and + 270°C at a heating rate of 10°C/min. The samples were first heated to 150°C at 30°C/min and then cooled down at 30°C/min before scanning to erase their thermal history. A nitrogen gas purge was applied, and the second heating curves were used for analysis.

Tapping-mode atomic force microscopy (AFM) studies were performed in a Discoverer TMX 2010 (TopoMetrix, Santa Clara, CA) microscope. Topography and phase image were obtained simultaneously with Si probes with a 20-nm nominal tip radius and with standard laboratory procedures.[27,28]

Simultaneous small-angle X-ray scattering (SAXS) and wide-angle X-ray scattering (WAXS) measurements of the films were performed at the SAXS-1 beamline at the National Laboratory of Synchrotron Radiation in Campinas, Brazil. A monochromatic beam of wavelength (λ) 1.488 Å was used, and the exposure time was 600 s. In the SAXS experiments, the scattering intensity was registered with a one-dimensional position-sensitive gas detector with a sample–detector distance of 1084.3 mm for values of the scattering vector ($\mathbf{q}$) of $0.009 < \mathbf{q} < 0.32$ [$\mathbf{q} = (4\pi/\lambda)\sin(\theta/2)$, where θ is the scattering angle]. We corrected the acquired data, subtracting the background contribution of the empty cell. The diffraction data were collected in a 2θ range from 10 to 80° with image plate detection and aluminum oxide (α-Al_2O_3) as a calibration standard.

The tensile properties (tensile strength, elongation at break, and tension at break) of the polymer films were measured at 25°C with an EMIC DL-3000 tensile testing machine (São José Pinhais, Brasil). Specimens were of the dog-bone test type with a 0.250-mm thickness, 6-mm width, and 33-mm length, according to the test procedure given in ASTM D 638 (Type IV specimen) and a speed of 500 mm/min.

Contact angle measurements were carried out with a Ramé-Hart goniometer (model 500, Netcong, NJ) with water as the probe liquid. All of the tests were performed on the air-facing surfaces of the samples. Measurements were performed on six different points to calculate the mean static contact angle (θ).

RESULTS AND DISCUSSION

Particle size and gel content results

The resulting products were stable dispersions with solid contents of about 30 wt %. Table III shows the particle size (by DLS) and gel fraction values of the systems prepared in this study. The decrease of particle size when the acrylic content increased was a consequence of the variable amount of added SDS (2 wt % acrylic monomer base).

The gel fraction for pure PU before polymerization was 0%, but after polymerization (PUpol), the crosslinking density increased because of the reaction of terminal double bonds. The gel fraction of AC polymer (0%) was in agreement with the synthetic method and the MMA/*n*-BuA ratio and was consistent with data reported in the literature.[29] The presence of PU increased the gel content for all of the samples to about 90%, regardless of the acrylic content This fact indicates that those PU/acrylate hybrids were crosslinked systems and explains the insolubility observed for these systems in normal solvents (e.g., tetrahydrofuran, dimethylformamide, dimethyl sulfoxide).

FTIR spectroscopy results

Figure 1 shows the FTIR spectra of PUpol, AC polymer, and the hybrid systems after cleaning. The

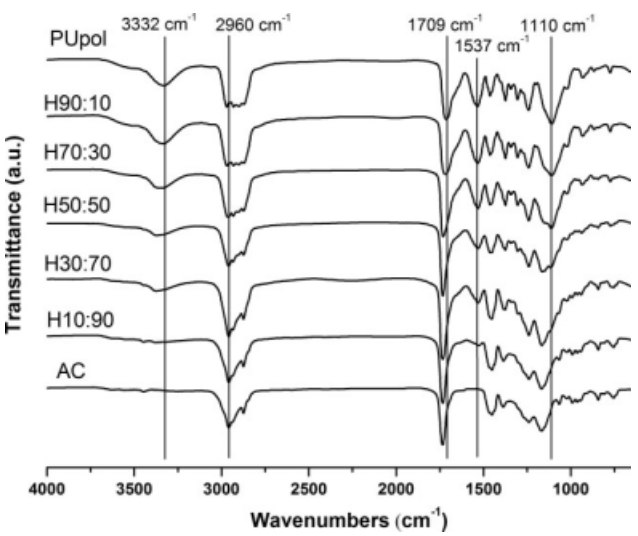

Figure 1 FTIR spectra of PUpol, AC, and the hybrid systems.

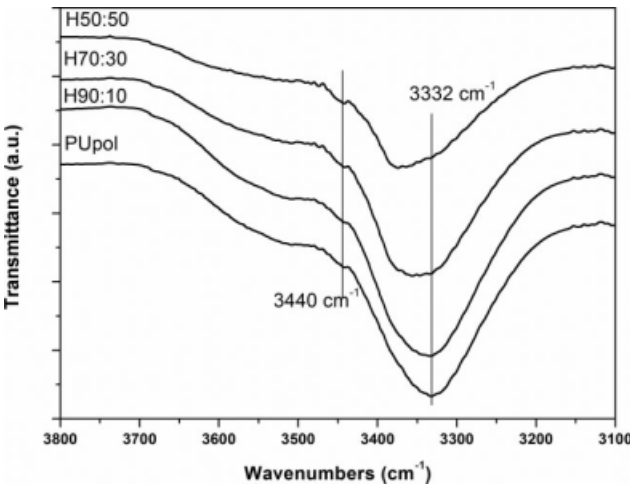

Figure 2 FTIR spectra in the N—H stretching region.

PUpol spectra showed typical bands corresponding to the HSs, where the absorption around 3332 cm^{-1} arose from the hydrogen-bonding N—H stretching vibration, whereas the free N—H stretching vibration appeared as a shoulder at about 3440 cm^{-1}. In addition, an absorption at 1537 cm^{-1} (a combination of C—N stretching and NH bending, amide II band), a broad band centered at 1709 cm^{-1} (free C=O and H-bonded C=O stretching), a signal centered at 1305 cm^{-1} (a combination of NH bending and C—N stretching), an absorption at 1239 cm^{-1} (a combination of NH bending and C—N stretching, amide IV band), and a band at 1110 cm^{-1} (C—O—C stretching vibration of polyetherdiol) were observed. Typical bands corresponding to SSs were also observed at 1373 cm^{-1} (bending of methyl groups), at 1457 cm^{-1} (antisymmetrical methyl bending and methylene scissoring), and from 2960 to 2875 cm^{-1} (saturated C—H stretching vibration bands).[30] The shoulder observed at about 3510 cm^{-1} was assigned to the OH stretching of the DMPA component. The spectrum of AC polymer (Fig. 1, bottom) showed a band at 1734 cm^{-1} assigned to carbonyl (C=O) stretching vibration of the acrylic ester groups and a band at 1168 cm^{-1} corresponding to the C—O stretching vibration. A progressive change in the spectrum was observed with increasing acrylic content, and the intensity of the acrylic C=O peak increased accordingly. A shift to higher wave numbers in the NH stretching bands was observed with increasing acrylic content; this arose from the breaking of hydrogen-bonding interactions (Fig. 2). The presence of the acrylic component changed; therefore, so did the hydrogen-bonding interactions. A low acrylic content (10 wt %) did not seem to be enough to modify this interaction, but acrylic contents of 30 wt % and higher shifted the maximum NH absorption band to a higher frequency characteristic of NH free-stretching vibrations.

TEM and TEM electron energy-loss spectroscopy results

Observation of the microstructure of colloidal particles was made by TEM. TEM images of the H90 : 10, H50 : 50, and H10 : 90 acrylic/PU hybrid particles are shown in Figure 3. For the H90 : 10 sample, a core–shell morphology was clearly observed. The TEM image of the H50 : 50 sample showed several particles, some of which showed core–shell morphologies similar to the H90 : 10 sample, but others showed no contrast at all. This indicated the presence of different types of particles. The same trend was observed when the acrylic content increased. Thus, in the H10 : 90, the same kinds of particles were observed (core–shell particles and homogeneous particles). Therefore, increasing the acrylic content favored multiple nucleation loci in the reaction media, and on the basis of the image analysis of samples with increasing acrylic contents, the

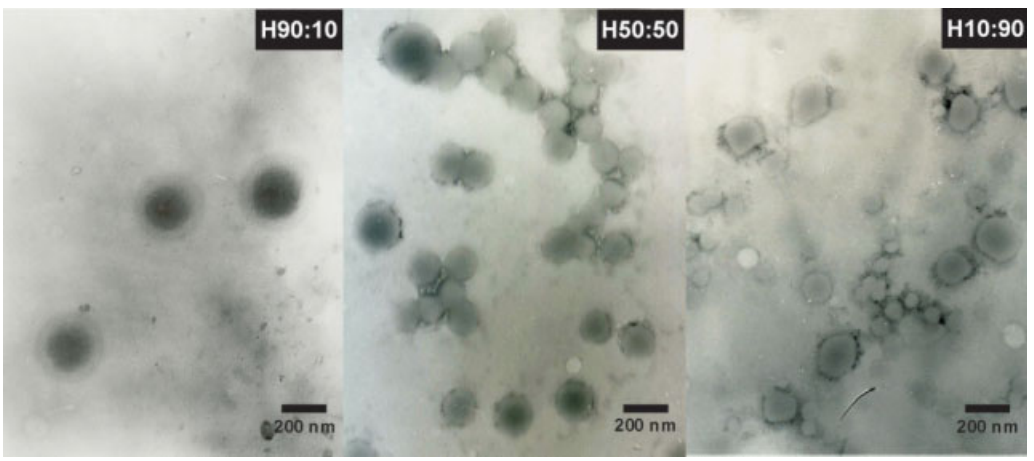

Figure 3 Typical TEM micrographs of the PU/acrylic hybrid systems. [Color figure can be viewed in the online issue, which is available at www.interscience.wiley.com.]

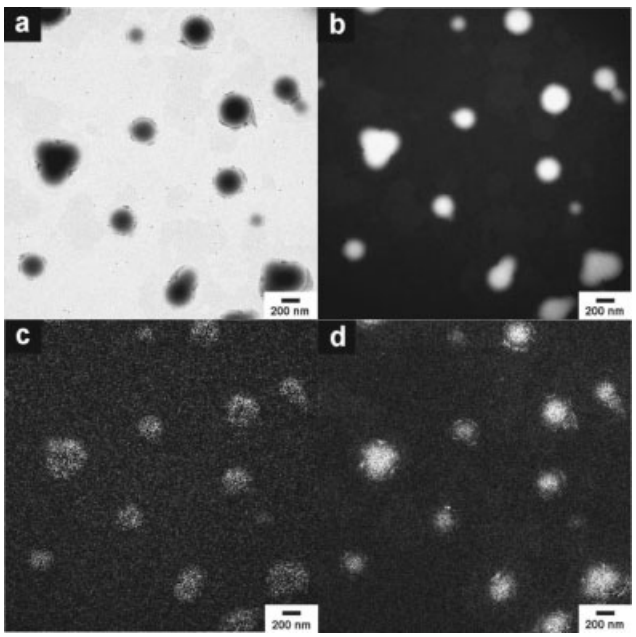

Figure 4 BF image obtained with monochromatic elastic electrons and energy-loss spectroscopy elemental maps of the H30 : 70 sample: (a) BF, (b) C, (c) N, and (d) S.

particles were the core–shell ones composed of PU and AC and homogeneous particles.

In agreement with previous studies, the acrylic component formed the core, and PU formed the shell.[7,16,17] This result was confirmed by electron energy-loss spectroscopy, where the contrast in the elemental maps revealed point-to-point particle composition variations and composition differences from one particle to another.[31] Bright-field (BF) and elemental map distributions of the H70 : 30 hybrid sample are presented in Figure 4. The micrographs are arranged in plates and display a standard BF image, together with element maps for all major latex constituent elements: C, S (from the initiator residues and surfactant), and N (from the polyurethanic polymer).

In the sample, the C map presented a uniform distribution of this element in the particles following a definite pattern. The particles in this map were the same size as the particles in the BF image. As carbon was the main element of the polymer, it was likely well distributed throughout the particle. As expected, adjacent particles displayed similar intensities because this was their main constituent element. This was different in N and S distribution maps. Although the N maps showed a homogeneous distribution of nitrogen in the particles, it also showed a lower density of this element in the particles compared to the C distribution. In addition, the larger particles showed a higher distribution of nitrogen in the outer portion of the particle; this indicated that this element had a higher concentration in this region. On the other hand, the S distribution maps for these particles also displayed a homogeneous distribution of sulfur inside the particles, which corresponded to the accumulation of this element in some domains. Because N represented the PU constituent and S was associated with the acrylic component, the results of the distribution maps suggest core–shell morphology for the larger particles, where the PU was in the shell and acrylic was in the core region.

On the other hand, the smaller particles displayed a uniform gray level in both the N and S distribution maps, without any evidence for local N or S accumulation within each particle. Although this was in accordance with previous TEM results, where smaller particles did not present a core–shell morphology [Fig. 3(b,c)], this indicated the coexistence of both PU and acrylic material within these particles.

DSC results

Figure 5 shows the DSC curves for PUpol and the AC copolymer, used as references, and the hybrid polymers. Typically, the PUs displays multiple transitions related to HSs and SSs. In this case, PUpol (Fig. 6, bottom) showed a glass transition of the SS around −30°C and an HS melting point around 160°C.[32–36] Another transition was observed around 35°C, but its origin was not completely understood. Therefore, additional thermal analyses, scanned at different rates, needed to be performed to elucidate the transition. Anyway, these results demonstrate the segmented nature of the PU, which was phase-separated into amorphous SS and partially crystalline HS domains. In addition, the pure AC polymer (Fig. 5, top) did not show a single glass-transition temperature (T_g); this proved that it did not have a homogeneous composition. Some composition drift may have occurred during the synthesis of the latex

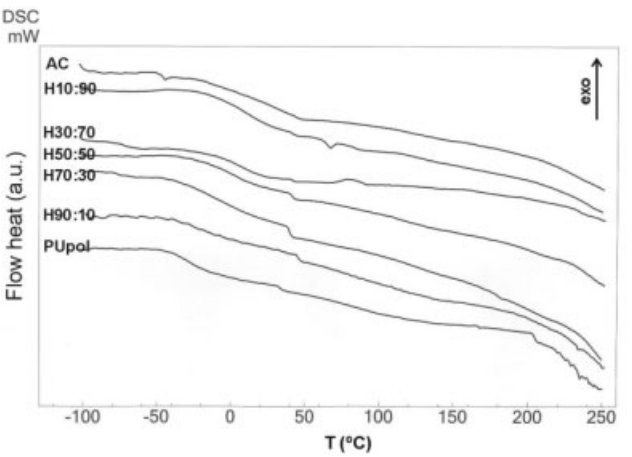

Figure 5 DSC curves for PUpol, AC, and the hybrid polymers.

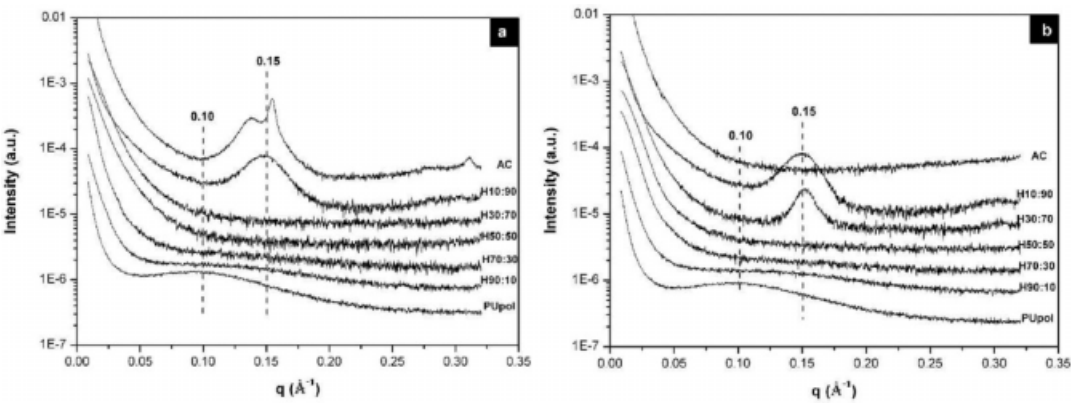

Figure 6 SAXS curves of PUpol and the acrylic polymer and hybrid systems (a) before and (b) after thermal curing.

because the polymerization involved a batch process, and the monomers had different reactivities in radical copolymerization. At least two transitions were observed: a sharp transition around −40°C and a broad transition at about 0°C; these transitions indicated the presence of two kinds of polymers with different compositions.[37,38] Thus, the lower T_g corresponded to a rich *n*-BuA copolymer, and the higher T_g corresponded to the mean composition of the copolymer in the sample. In Figure 5, it is possible to observe a progressive change in the curves with increasing acrylic content. As the acrylic content increased in the systems, there was a broadening of the SS glass transition of the PU. The reason for this behavior resulted from the lower flexibility of the SSs and their interaction with HSs or acrylic chains. In the H50 : 50 sample, the glass transition of the SS and transitions related to the HS were negligible; this indicated that, according to the DSC technique, this sample behaved like a homogeneous material, although the TEM data previously discussed showed that particles in this sample were of the core–shell types.[9,39,40] However, an important change occurred when the acrylic content increased to 70 and 90 wt %. In H30 : 70, a weak transition appeared around 81°C, and in H10 : 90, a well defined transition appeared around 60°C, neither of which were observed in samples with lower acrylic contents. This additional transition suggested that, at the H10 : 90 composition, segregation occurred and led to the presence of acrylic domains. The HS melting point observed in PUpol was no longer observed in the hybrid systems; this indicated that the acrylic chains modified the HS ordering.

SAXS and WAXS results

SAXS experiments yield information on the segregation of phases of different electron densities within a sample. Of primary importance are (1) the interdomain spacing (or *d*-spacing), which may be correlated with domain size, and (2) the interfacial thickness, which may be used to correlate the chemistry and structure. Figure 6 shows the scattering intensity versus **q** for pure PU and the acrylic polymers and hybrids with different acrylic contents before and after thermal curing. The SAXS spectrum of pure PU showed the typical broad central maximum at about 0.1 $Å^{-1}$ due to microphase separation between the hard and soft domains composing the PU chains.[41] The pure acrylic sample, on the other hand, displayed two peaks at about 0.137 and 0.154 $Å^{-1}$ after film formation at room temperature, which were related to the presence of the interface between latex particles and the tendency of acrylic acid to form local crystalline domains. Neither peak was observed after curing at 60°C [see Fig. 6(b)], in agreement with the T_g of the acrylic polymer, where a general coalescence of latex particles after curing was expected, therefore, loosing the interface between particles and the domains of acrylic acid. Because of the high mobility of the PU chains, the morphology after film formation at room temperature of this sample did not change after curing and reached almost complete coalescence at room temperature. The incorporation of the acrylic component reduced the intensity of the maximum at 0.1 $Å^{-1}$ observed in the pure PU polymer. Increasing the acrylic content reduced the intensity even more [Fig. 6(a)], and interestingly enough, a featureless spectrum was observed for 50 wt % acrylic content in both the cured and uncured samples. This indicated a high degree of phase mixing or a very homogeneous matrix at the nanoscale level. However, in the sample containing 70 wt % acrylic component, a peak in **q** at about 0.15 $Å^{-1}$ appeared after curing. This type of SAXS curve is attributed to a two-phase system with sharp boundaries and with electron density contrast and indicated phase separation in this particular composition. At 90 wt % acrylic content, phase separation was observed in both the cured and uncured samples. From a synthetic point

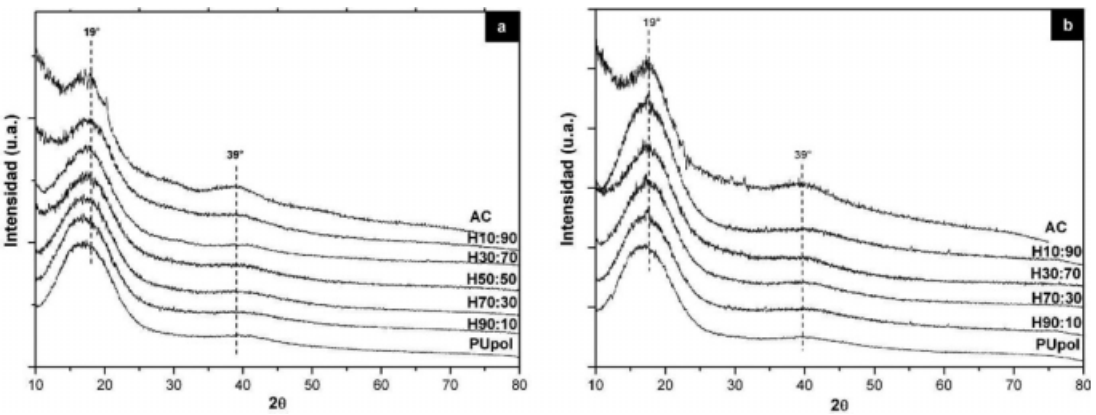

Figure 7 WAXS curves of PUpol and the acrylic polymer and hybrid systems (a) before and (b) after thermal curing. The curves were shifted on the *y* axis by an arbitrary amount for clarity.

of view, during the emulsion polymerization in systems with acrylic contents of up to 50 wt %, the PU particles swelled completely, and copolymerization took place with the acrylic monomer inside the particles. The presence of the acrylic component influenced the crystallization process during film formation, and the broad band observed in the pure PU spectrum was not observed anymore. When the acrylic content was increased, part of the acrylic monomers was not incorporated into the particles, and in addition to the PU/AC hybrid particles, latex particles of the pure acrylic polymer were also formed during polymerization, which, in turn, segregated during film formation. As expected, thermal curing facilitated phase separation. The positions of the correlation peaks corresponded to those typical of this length of sample. The interdomain repeat distance (L), defined as the average distance between two hard domains, was obtained from SAXS intensity profiles by the application of Bragg's equation:[42]

$$L = 2\pi/q^*$$

where q^* is the observed peak position in the SAXS curve.

Thus, the interdomain spacing in pure PU was about 6.3 nm; this indicated that IPDI promoted hydrogen-bond formation and efficient packing in the hard domains. The incorporation of the acrylic polymer seemed to modify this situation by decreasing the intensity of the scattering and eliminating peaks in the hybrid systems with intermediate acrylic content. The observed peaks with 90 wt % acrylic content at about 0.15 Å^{-1} corresponded to a smaller interdomain distance of 4.2 nm. The interdomain spacing, specific for this composition, may have resulted from the presence of acrylic segments and, therefore, formed a two-phase system.

To investigate the underlying microstructure of PU with different acrylic contents, in addition to SAXS, WAXS was used. As shown in Figure 7 (the spectra were shifted for clarity), all samples showed similar WAXS curves with wide diffraction halos around 19 and 39°, which are typical for amorphous polymeric materials, because the molecular chain distance in noncrystalline materials is about 0.4–0.5 nm.[43] The first halo was very wide and gave evidence for the presence of a poorly ordered phase with looser packing. After curing, diffuse crystalline scattering peaks for samples with a higher acrylic content were observed. By a close analysis of Figure 7(a) (samples before thermal annealing), a slight shift to higher 2θ values of the peak at 19° was observed when the acrylic content increased. An increase in the overall intensity for $2\theta < 15°$ was also observed; this followed the same trend. Additionally, a weak contribution appeared at $2\theta = 30°$ in the pure acrylic sample. However, thermal treatment of the samples promoted changes in the morphology and in the WAXS curves as well, especially in the sample with 90 wt % acrylic content. The narrow shift previously observed and the shoulder at $2\theta < 15°$ were no longer present after curing. In this case, a sharp peak appeared on the broad peak at 19°, probably due to the distinction between the PU and AC phases at this scale after curing.

AFM results

Phase contrast in tapping-mode AFM is determined by the topographic, viscoelastic, and adhesive properties of samples. It is a powerful tool that provides micrometer/nanometer-scale information about the surface structure. Under the phase setting we used, low-modulus soft regions appeared as brighter tones, whereas high-modulus hard regions were darker. Figures 8 and 9 show the topography and viscoelastic behavior of samples H70 : 30 and H30 : 70, respectively, before and after annealing. These samples were taken as representative of the two

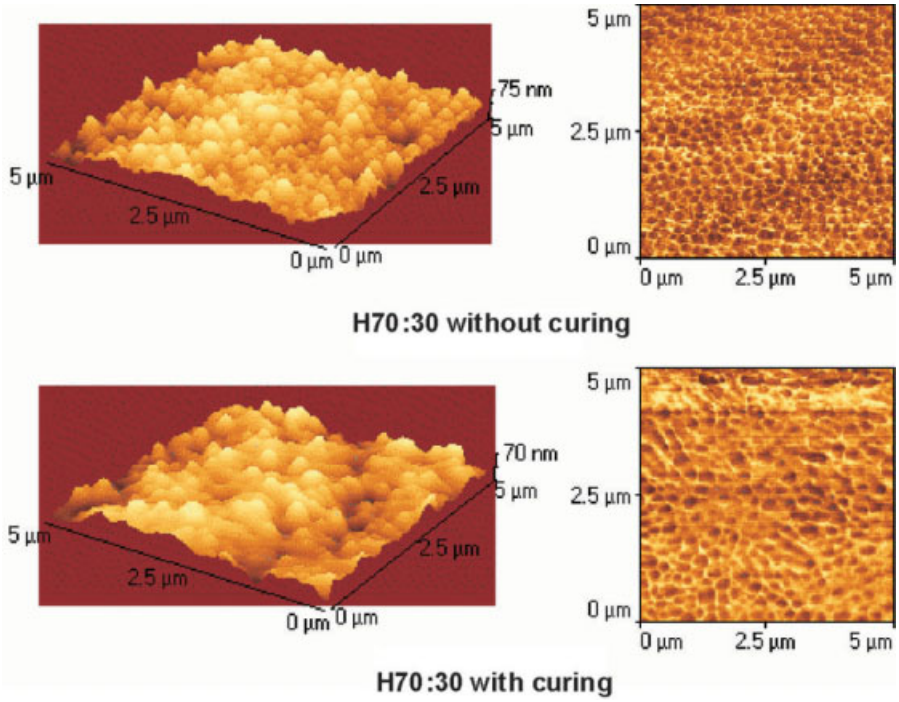

Figure 8 Topography and respective phase-contrast image of the H70 : 30 sample before (top) and after (bottom) thermal annealing. [Color figure can be viewed in the online issue, which is available at www.interscience.wiley.com.]

systems with different behaviors, on the basis of the SAXS data previously discussed in this article. Before annealing, a close packing of the particles was observed in both samples. Topography pictures clearly showed the shape of the latex particles of both as-cast films, where particles from H70 : 30 were bigger than particles from H30 : 70; this was in agreement with the TEM results and the particle sizes obtained by DLS measurement. In the phase-contrast images, the films displayed hard-phase domains in a soft matrix. Profiles in different regions of each film were used to determine the average

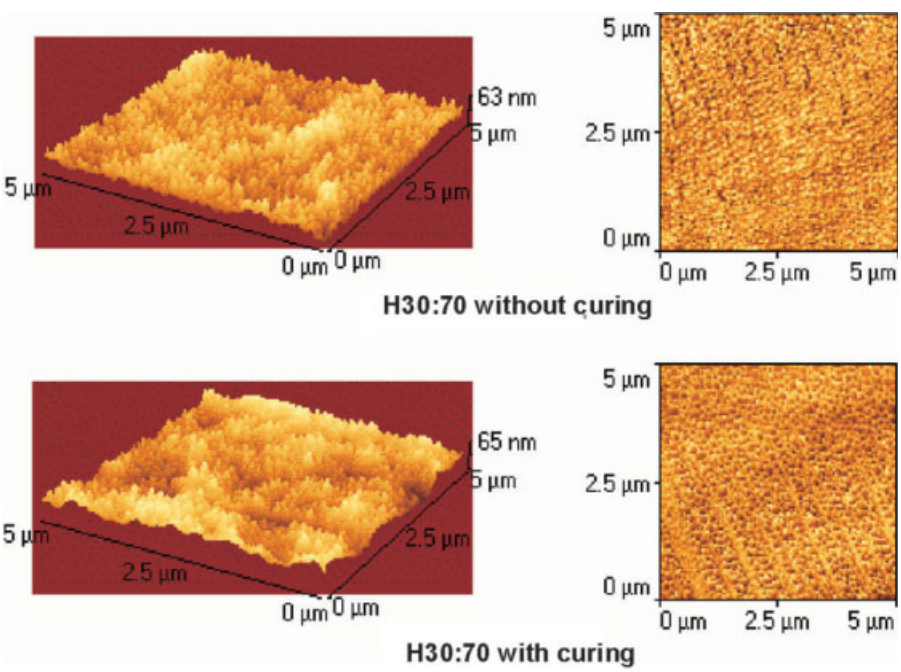

Figure 9 Topography and respective phase-contrast image of the H30 : 70 sample before (top) and after (bottom) thermal annealing. [Color figure can be viewed in the online issue, which is available at www.interscience.wiley.com.]

hard-domain size. The regular distribution of the hard domains in the film supported the proposition that the acrylic polymerization occurred within the urethane particle; this was in agreement with the TEM observations. Consequently, results demonstrate that the structure of the single particles was maintained during film formation, and this determined the film structure. After annealing, topography showed a more coalesced film as compared to the uncured sample for H70 : 30; the particles were flattened, and interdiffusion was observed in the phase-contrast image for this hybrid sample.[44] On the other hand, sample H30 : 70 was similar to the uncured sample; this indicated that the thermal treatment did not improve the packing of the hybrid particles in the film. However, the shape and morphology of the latex particles were still clearly visible in the surface morphology after annealing. This suggested that the morphology was preserved at this scale, even after curing. A close examination of the cured 30 : 70 sample revealed some stripes, which could be tentatively explained as some sort of particle segregation during the annealing of the sample.

Mechanical properties results

In this section, the stress–strain response, extent of stress relaxation, and mechanical behavior of the pure and hybrid polymers are presented and compared. Figure 10 shows the stress versus strain curves of the films before curing of PUpol, AC, and the PU/acrylate hybrids. Curves for the samples after curing are not included for simplicity, but similar behavior was observed. Table IV displays the elastic modulus (Young's modulus), and elongation and stress at break values of the cured and uncured films. The pure acrylic polymer sample showed a yield point at a very low elongation with a stress peak and then a minimum in the curve followed by a strain-hardening phenomenon. The presence of a yield point is characteristic of a two-phase structure.[45] The maximum stress was close to 10 MPa, and the elongation at break was about 500%. On the other hand, no distinct yield point was observed for PUpol and samples with 10 and 30 wt % acrylic; this indicated that these systems had a one-phase structure. Samples containing more than 50 wt % acrylic behaved more similarly to pure acrylic with comparable elongation at break values, and they displayed rubbery behavior in the tested conditions. All of these results were consistent with the morphology SAXS results and indicated that, for high acrylic contents, the acrylic phase acted as a continuous matrix with soft (hybrid) inclusions. Although all of the parameters increased with thermal treatment for the cured samples, an interesting effect was observed for both the elongation at break and breaking stress. Increases in both of these parameters were notable for the H50 : 50 with curing, but they were less important for H30 : 70 and H10 : 90. As in the SAXS results, these samples again showed different behavior, and this was probably related to changes in the morphology of the polymers. The first systems of the series, with 10, 30, and 50 wt % acrylic component (H90 : 10, H70 : 30, and H50 : 50, respectively), behaved like homogeneous materials, which, after thermal annealing, improved the chain packing and formed a much more regular structure. In a different way, the samples with higher acrylic contents (H30 : 70 and H10 : 90) behaved like phase-separated systems, and thermal treatment did not change their morphology. This was the reason why the tensile properties of the last group were not affected to the same degree as the first group. These significant changes in the elastic modulus and the breaking stress after thermal treatment were due to the formation of an extended polymeric network. The

TABLE IV
Parameters Obtained from the Stress Versus Strain Curves of Pure PUpol, AC, and the Hybrid Systems Before and After Thermal Curing

	Elongation at break (%)		Modulus (MPa)		Stress at break (MPa)	
Sample	bc	ac	bc	ac	bc	ac
PUpol	244	257	87.7	108.1	17.9	22.2
H90 : 10	227	289	68.5	83.7	14.5	23.3
H70 : 30	249	244	49.6	66.9	11.4	15.1
H50 : 50	268	369	21.8	22.0	7.4	14.1
H30 : 70	420	421	10.9	11.2	9.2	9.2
H10 : 90	490	518	49.6	54.0	10.1	12.1
AC	505	535	103.9	112.7	10.3	13.6

bc = before curing; ac = after curing.

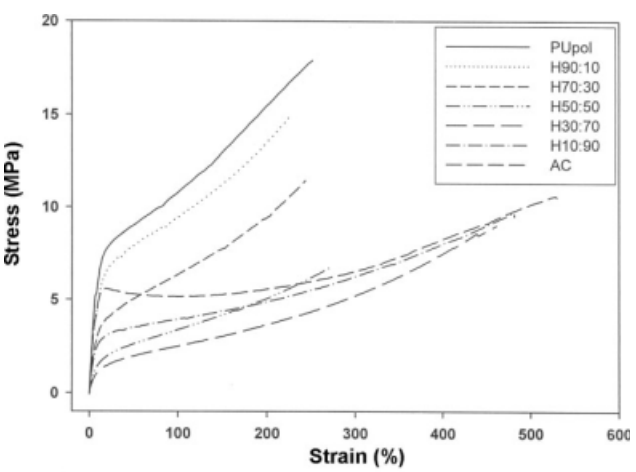

Figure 10 Stress versus strain curves of PUpol and the acrylic polymer and hybrid systems before thermal annealing.

TABLE V
Contact Angle, Roughness, and Buchholz Hardness Values of the Films Before and After Thermal Annealing

	Conctact angle (°)		Roughness (mm)		Buccholz hardness	
Sample	bc	ac	bc	ac	bc	ac
PUpol	62.49	64.03	0.11	0.20	38	51
H90 : 10S	62.14	65.58	0.64	0.47	47	50
H70 : 30S	63.26	67.23	2.72	0.85	33	38
H50 : 50S	72.93	75.09	3.54	1.90	27	28
H30 : 70S	63.24	50.27	1.71	1.45	27	28
H10 : 90S	62.15	50.31	0.74	0.30	33	34
AC	57.41	38.28	0.27	0.31	34	48

bc = before curing; ac = after curing.

nonlinear behavior described here, with increasing acrylic content, was previously observed by Kukanja et al.[10] However, the systems studied by Kukanja et al.[10] were slightly different, and we did not expected to have the same conclusions. Regardless of these dissimilarities, the PU/AC hybrids presented nonlinear behavior as the acrylate content increased.

In addition to effects at scales larger than the domain structure, the hard-domain cohesion can also influence the mechanical properties.[46] The incorporation of SSs in the HS domain would be expected to reduce the HS domain cohesion. In this case, the incorporation of 10–50 wt % acrylic content probably affected the HS domain cohesion and reduced the mechanical properties. At higher acrylic compositions (>50 wt %), the most likely morphology, as suggested by SAXS, was of the two-phase type, with a continuous acrylic phase and the hybrid polymer as the second separated phase; this would explain the similar behavior of the H30 : 70 and H10 : 90 samples and the pure acrylic polymer.

Water contact angle, roughness, and Buchholz hardness results

To investigate the surface properties of the hybrid materials, water contact angle, roughness, and Buchholz hardness measurements were performed (Table V). Before thermal curing, the PU film had a fairly polar surface and showed a water contact angle of 62.5°. The contact angles increased with acrylic contents up to 50 wt %. At higher acrylic contents, this parameter changed up to the value of the acrylic polymer. The cured samples presented similar behavior, with a slight increase in the contact angle for samples up to 50 wt %; a notable decrease was observed for the rest of the samples. Again, the sample with 70 wt % acrylic content behaved differently and did not follow the trend observed for the other samples; this indicated a change in morphology for this composition, in agreement with the SAXS results and observed stress–strain properties.

The roughness increased as the acrylic content increased up to 50 wt %, with a maximum at this composition. After that, the roughness decreased down to the acrylic extreme. The cured samples followed the same trend observed in the uncured samples, but in this case, the roughness values were smaller; this indicated that thermal annealing produced coalescence. The Buchholz hardness results showed a minimum around 50 wt %/70 wt % acrylic content (before and after curing), in agreement with the modulus results presented previously with the mechanical properties' results. Small differences were observed after thermal annealing, except for in the PUpol and AC systems, which probably had increased Buchholz hardness because these systems improved the chain packing.

Importantly, the nonlinear behavior of the properties for these systems, which presented an inflexion point at around 70 wt % acrylic content, was probably related to the morphology changes in the hybrid systems after the particle composition changed.

CONCLUSIONS

Water-based PU/acrylate dispersions were synthesized and characterized to investigate the effects on morphology and mechanical properties of the variation of the acrylic content in a broad range. The incorporation of different amounts of acrylic components in PU and the formation of a hybrid material changed the morphology of the original PU and, therefore, the final properties. The acrylic monomers reacted with the PU prepolymer double bonds, altered the HS distribution, and inhibited the microphase separation typically found in pure PU. The SAXS data suggested that, beyond the usual microphase separation between SSs and HSs in the PUs, phase separation might also have occurred within soft domains, specifically for the acrylic polymer, because of some degree of incompatibility between them. Depending on the application required, as much as 50 wt % acrylic was incorporated without a loss of the excellent properties of PUs. However, to obtain a homogeneous material, the incorporation of acrylics should be performed with a suitable pathway, such as that described in this article, to obtain chemical bonds between both polymers. Physical blends do not have the same properties as the hybrid systems described in this article; therefore, the comparison of these two systems will be the subject of a future article.

The authors thank L. Gambino for his technical assistance and Christopher Young for his assistance in reviewing and

correcting the article. Two of the authors (J.I.A. and O.R.P.) are members of Comisión de Investigaciones Científicas (CIC), Provincia de Buenos Aires (Argentina). One of the authors (P.J.P.) is a postdoctoral fellow of CONICET (Argentina), and one of the authors (P.S.A.) is a doctoral fellow of Agencia Nacional de Promoción Científica y Tecnológica. One of the authors (F.G.) thanks Conselho Nacional de Desenvolvimento Científico e Tecnológico (Brazil) for their support through the INCT (National Institutes for Science and Technology) program.

References

1. Król, P. Prog Mater Sci 2007, 52, 915.
2. Coogan, R. G.; Bilancieri, J. J.; Pollano, G. Am Paint Coat J 1994, 78, 49.
3. Tennebroek, R.; Geurts, J.; Overbeek, A.; Harmsen, A. Eur Coat J 1997, 11, 1016.
4. Okamoto, Y.; Hasegawa, Y.; Yoshino, F. Prog Org Coat 1996, 29, 175.
5. Kim, J. Y.; Suh, K. D. Colloid Polym Sci 1996, 274, 920.
6. Kim, B. K.; Lee J. C. J Appl Polym Sci 1995, 58, 1117.
7. Hirose, M.; Kadowaki, F.; Zhou, J. Prog Org Coat 1997, 31, 157.
8. Hegedus, C. R.; Kloiber, K. A. J Coat Technol 1996, 68, 39.
9. Otts, D. B.; Dutta, S.; Zhang, P.; Smith, O. W.; Thames, S. F.; Urban, M. W. Polymer 2004, 45, 6235.
10. Kukanja, D.; Golob, J.; Krajnc, M. J Appl Polym Sci 2002, 84, 2639.
11. Brown, R. A.; Coogan, R. G.; Fortier, D. G.; Reeve, M. S.; Rega, J. D. Prog Org Coat 2005, 52, 73.
12. Zhang, H. T.; Guan, R.; Yin, Z. H.; Lin, L. J Appl Polym Sci 2001, 84, 2639.
13. Wang, C.; Chu, F.; Graillat, C.; Guyot, A.; Gauthier, C.; Chapel, J. P. Polymer 2005, 46, 1113.
14. Wang, C.; Chu, F.; Guyot, A.; Gauthier, C.; Boisson, F. J Appl Polym Sci 2006, 101, 3927.
15. Dimonie, V. L.; Daniels, E. S.; Shaffer, O. L.; El-Aasser, M. S. In Lovell, P. A.; El-Aasser, M. S., Eds.; Emulsion Polymerization and Emulsion Polymers; Wiley: New York, 1997; p 293.
16. Hirose, M.; Zhou, J.; Nagai, K. Prog Org Coat 2000, 38, 27.
17. Guyot, A.; Landfester, K.; Schork, F. S.; Wang, C. Prog Polym Sci 2007, 32, 1439.
18. Wang, C.; Chu, F.; Graillat, C.; Guyot, A. Polym Adv Technol 2005, 16, 139.
19. Wang, C. B.; Cooper, S. L. Macromolecules 1983, 16, 775.
20. Speckhard, T. A.; Hwang, K. K. S.; Lin, S. B.; Tsay, S. Y.; Koshiba, M.; Ding, Y. S.; Cooper, S. L. J Appl Polym Sci 1985, 30, 647.
21. Smith, T. L.; Dickie, R. A. J Polym Sci Part C: Polym Symp 1969, 26, 163.
22. Amalvy, J. I. Pigment Resin Technol 2002, 31, 275.
23. Pardini, O. R.; Amalvy, J. I. J Appl Polym Sci 2008, 107, 1207.
24. Aznar, A. C.; Pardini, O. R.; Amalvy, J. I. Prog Org Coat 2006, 55, 43.
25. Amalvy, J. I.; Percy, M. J.; Armes, S. P.; Leite, C. A. P.; Galembeck, F. Langmuir 2005, 21, 1175.
26. Valadares, L. F.; Leite, C. A. P.; Galembeck, F. Polymer 2006, 47, 672.
27. Rippel, M. M.; Leite, C. A. P.; Lee, L. T.; Galembeck, F. J Colloid Interface Sci 2005, 288, 449.
28. Braga, M.; Costa, C. A. R.; Leite, C. A. P.; Galembeck, F. J Phys Chem B 2001, 105, 3005.
29. González, I.; Asua, J. M.; Leiza, J. R. Polymer 2007, 48, 2542.
30. Irusta, L.; Fernández-Berridi, M. J. Rev Plast Mod 1999; 78, 245.
31. Amalvy, J. I.; Asua, J. M.; Leite, C. A. P.; Galembeck, F. Polymer 2001, 42, 2479.
32. Heijkants, R. G. J. C.; van Calck, R. V.; van Tienen, T. G.; de Groot, J. H.; Buma, P.; Pennings, A. J.; Veth, R. P. H.; Schouten, A. J. Biomaterials 2005, 26, 4219.
33. Mondal, S.; Hu, J. L. J Membr Sci 2006, 274, 219.
34. Koberstein, J. T.; Galambos, A. F. Macromolecules 1992, 25, 5618.
35. Jeong, H. M.; Lee, S. Y.; Kim, B. K. J Mater Sci 2000, 35, 1579.
36. Camberlin, Y.; Pascault, J. P.; Letoffe, J. M.; Claudy, P. J Polym Sci Part A: Polym Chem 1982, 20, 1445.
37. Haibo Yu, H.; Peng, J.; Zhai, M.; Li, J.; Wei, G.; Qiao, J. Rad Phys Chem 2007, 76, 1746.
38. Meseguer Dueñas, J. M.; Torres Escuriola, D.; Gallego Ferrer, G.; Monleón Pradas, M.; Gómez Ribelles, J. L.; Pissis, P.; Kyritsis, A. Macromolecules 2001, 34, 5525.
39. Baek, S. H.; Kim, B. S.; Kim, B. K. Prog Org Coat 2004, 49, 353.
40. Król, P.; Król, B.; Pikus, S.; Skrzypiec, K. Colloid Surf A 2005, 259, 35.
41. Bolze, J.; Ballauff, M.; Rische, T.; Rudhardts, D.; Meixner, J. Macromol Chem Phys 2004, 205, 165.
42. Pattanayak, A.; Jana, S. C. Polymer 2005, 46, 5183.
43. Kumar, H.; Siddaramaiah; Somashekar, R.; Mahesh, S. S. Mater Sci Eng A 2007, 447, 58.
44. Barrère, M.; Landfester, K. Macromolecules 2003, 36, 5119.
45. Mohammed, S.; Daniels, E. S.; Sperling, L. H.; Klein, A.; El-Aasser, M. S. J Appl Polym Sci 1997, 66, 1869.
46. Speckhard, T. A.; Cooper, S. L. Rubber Chem Technol 1986, 59, 405.